SINERGI Vol. 28, No. 3, October 2024: 567-584
http://publikasi.mercubuana.ac.id/index.php/sinergi
http://doi.org/10.22441/sinergi.2024.3.013

A review analysis of corrosion rate on stainless steel pipe in sea water media

Muhammad Alfattah[1]*, I Gusti Ayu Arwati[1], Edy Herianto Majlan[2]
[1]Department of Mechanical Engineering, Faculty of Engineering, Universitas Mercu Buana, Indonesia
[2]Fuel Cell Institute, Universiti Kebangsaan Malaysia, Malaysia

Abstract
Regarding providing energy, few sectors are as massive as the oil and gas business. One of the most crucial parts of oil and gas production is the distribution pipes or pipelines that transport the production fluids, which include oil and gas, from one distribution point to another. The corrosion of A316 material, which can lead to holes or pitting, and the damage it causes in most industrial operations, particularly in the oil and gas industry, has resulted in substantial losses at high prices over an extended period of time. In the study, we will quickly examine what corrosion is, the different kinds of corrosion, inhibitors, and how to assess the corrosion rate of A316 stainless steel in salt water. Analysis of the electrochemical corrosion rate of Inconel 600 nickel alloy and stainless steel 316L subjected to varying amounts of saltwater (freshwater, seawater, mixed water). Because chlorine speeds up corrosion, alloys like Inconel 600 and 316L undergo pitting corrosion. The molybdenum component gives 316 stainless steel its superior corrosion resistance. That's why it works well for gas and oil pipelines that go through saltwater. Nevertheless, materials exposed to maritime environments must have cathodic protection or coating to prolong their life and stop the pipe from continuously corroding.

Keywords:
Electrochemical Corrosion;
Oil and gas pipe;
Pitting Corrosion;
Sea Water Environment;
Types of Inhibitors;

Article History:
Received: November 28, 2023
Revised: February 4, 2024
Accepted: February 24, 2024
Published: October 2, 2024

Corresponding Author:
Muhammad Alfattah
Mechanical Engineering Department, Universitas Mercu Buana, Indonesia
Email: 21fattah21@gmail.com

INTRODUCTION

With deposits located over nearly the whole country, Indonesia is one of the world's leading oil and gas producers [1]. One of Indonesia's primary sources of revenue, mining has been around since the country's inception [2]. It is possible to find oil off the coast of this nation [3]. There are a lot of operating costs associated with mining, and the process itself is fairly costly [4]. The placement of pipes in different conditions, including salt water, is one method of oil distribution [5]. The pipe is a crucial component of the oil and gas extraction process, carrying gas from the well to the processing plant. The next step is to refine the oil and gas before selling it [6]. Proper maintenance of oil and gas pipelines is critical to ensuring their proper usage and longevity [7].

Because of the harsh conditions found in salt water, the materials used to construct petroleum pipelines must be able to withstand the corrosive and abrasive elements found in the water [8][9]. Stainless steel 316 or 316L is the material of choice for pipes in the oil and gas sector [10][11]. Because it contains molybdenum, stainless steel 316 is very resistant to corrosion [12][13].The mechanical characteristics, corrosion resistance, weldability, and carbon content of stainless steel 316 and 316L are distinct from one another [14]–[16].

Corrosion is a major threat to offshore installations in the maritime environment, and it may lead to a number of incidents, including pipe damage [17][18]. The corrosion of A316 stainless steel can be caused by a variety of circumstances, such as Sodium chloride (NaCl) can induce pitting corrosion when present [19][20]. Environments containing extremely high concentrations of salt (chloride) are prone to pitting corrosion [21][22].

Pitting can occur when stainless steel A316 comes into direct touch with saltwater, which is a common problem in marine applications [23]. Therefore, to guarantee the pipe's longevity and safety during its operational term, it is important to plan and assess the pipe's strength and appropriateness [24]. Cathodic protection technologies and other preventative measures are required to stop pipes from corroding continuously [25].

The study's overarching goal is to provide a concise description of corrosion, its many forms, inhibitors for these forms, and a method for measuring the corrosion rate of A316 stainless steel in saltwater environments.

CORROSION STUDIES

Corrosion is the degradation of material properties due to chemical or electrochemical reactions with the environment, and in many cases means electrochemical oxidation of metals.

Table 1 shows corrosion studies, Table 2 description of the types of corrosion in A316 material. Description of the yypes of corrosion in inconel 600 material, as presented in Table 3, Table 4 shows corrosion behavior 316l in sea water and artificial sea water, Table 5 shows corrosion behavior inconel 600 in sea water and artificial sea water.

Here we will go over the several elements that might cause 316 stainless steel to corrode, as well as how to prevent it from happening. Pitting corrosion can occur when sodium chloride (NaCl) is present. In chloride conditions, pitting corrosion and crevice corrosion can occur [28].

Table 1. Corrosion Studies

No	Corrosion Studies	Reference	Author Analysis
1	Electrochemical oxidation of metals is a common example of corrosion, which is the loss of material characteristics caused by environmental chemical or electrochemical interactions.	[26]	Deterioration of material qualities, often known as corrosion or rust, can be caused by a number of environmental conditions, including water content, soil resistivity, pH, dissolved oxygen, temperature, and microbiological activity. Damage to equipment, machinery, and building structures can occur both directly and indirectly as a result of corrosion.
2	The material impacted by corrosion, also known as rust, can degrade and have its lifespan reduced as a result of corrosion. One of the biggest issues facing the industrial world is corrosion.	[27]	
3	Numerous studies have examined the causes of corrosion, particularly in relation to the oil and gas sector. These studies have concentrated on the primary methods for assessing crucial environmental factors and dissolved oxygen limits, with a particular emphasis on stainless steel. Among these environmental factors, temperature, chloride, and oxygen concentrations rank highest, along with the configuration of the component or assembly in question.	[28]	
4	In order to determine the model used for sizing metal structures, which is buried in the design stage, it is necessary to compute the sequence of features fluctuations that cause corrosion. Practices will increase the reliability of the developed model based on the data sets that flow into it. Using a combination of his book, corrosion tests, and standards, Baboian establishes the dependability level of corrosion data.	[29]	
5	Equipment, machinery, and building structures can suffer direct losses as well as indirect damages due to rust.	[30]	
6	Hydrogen concentration, soil resistance, acidity, temperature, dissolved oxygen, and microbes all have a role in corrosion. The corrosive quality of the soil is the primary cause of metal pipe corrosion. Because of the presence of sulfate, chloride, moisture, and bacterial activity, the corrosive qualities of land are increased.	[31]	
7	Impurities, air, temperature, and the composition of the metal, as well as environmental elements like salt, can all contribute to corrosion. Understanding the processes that suppress corrosion is crucial for designing, life cycle managing, and economically viable these systems.	[32]	
8	Depending on the particular microorganism/material/electrolyte interaction, microalgae, fungus, bacteria, and archaea can either directly or indirectly affect corrosion.	[33]	

Table 2. Description of The Types of Corrosion in A316 Material

No.	Type of Corrosion	Description
1	Pitting Corrosion	Among corrosions, pitting corrosion is among the most common and harmful [34]. In chloride conditions, structural elements like stainless steel are severely damaged by corrosion. Small metal surfaces corrode easily and develop holes or cavities as a result of localized corrosion (pits) [33, 34, 35, 36].
2	Uniform Corrosion	Among the many types of corrosion that can develop on metal surfaces due to atmospheric interaction is uniform corrosion. The has little effect on the substance and disperses evenly throughout it [39][40]. Uniform corrosion is caused by changes in the mechanics, geometry, and chemical characteristics of the structural components. It should be noted that corrosion is primarily caused by the spread of damaged layers, and the rate at which the corrosion proceeds is influenced by environmental factors [41].
3	Stress Corrosion Cracking	Corrosion under stress Cracking occurs when a corrosive environment and tensile stress work together to initiate and propagate cracks in metals that are sensitive to the process [42]. When compared to other forms of corrosion, stress corrosion cracking stands out. Stress corrosion is thought to be caused by a multitude of variables that impact the specific kind of corrosion, including chemical make-up and soil moisture, climate, temperature fluctuations, vibrations, and substantial levels of residual stress. diagonal axial fissures. Steel corrosion cracking can start on the surface and progress deeper into the metal [43][44].
4	Galvanic Corrosion	One kind of corrosion that may happen on the anodic side of a pair is galvanic corrosion, which, according to Faraday's law, is directly linked to galvanic current. A current known as galvanic current runs from one material to another when two electrically conducting materials in close proximity to one other are exposed to an electrolyte [45]. Welding several stainless steels together causes galvanic corrosion [39].
5	Crevice corrosion	When one metal surface comes into touch with the bulk electrolyte and another surface is exposed to the electrolyte that is trapped and stagnant in a "crevice," a specific kind of localized corrosion called crevice corrosion happens. When depassivation agents, primarily chloride, are present, passive metal crevice corrosion happens at temperatures and potentials above critical, while non-passive corrosion, also known as corrosion under deposits, happens in an environment that is not specific to the metal because the metal is actively corroding [39][46][47]. Corrosion in small spaces created by metal-on-metal or metal-on-nonmetal contacts was first described as crevice corrosion. The form of corrosion is particularly significant in very corrosion-resistant materials, such industrial nickel alloys and stainless steel 316 (or 316L) [48].
6	Erosion Corrosion	Erosion factors, such as particle size, impact angle, and flow velocity, affect the rate of surface erosion of austenitic stainless steel [49]. The oil and gas sector ranks erosion corrosion among the five most common types of damage processes. Solid particles in the slurry gradually mechanically remove material from exposed surfaces, while electrochemical corrosion reactions take place on metal surfaces. The complicated phenomena is known as erosion corrosion. A material's microstructure affects its mechanical and electrochemical characteristics, which in turn govern its corrosion-erosion behavior [50][51].

Table 3. Description of The Types of Corrosion in inconel 600 Material

No	Type of Corrosion	Description
1	Stress Corrosion Cracking	Cracks can form and spread in metals that are vulnerable to stress corrosion cracking when a corrosive environment and tensile stress work together [42]. Concerning the safety of structures, stress corrosion cracking (SCC) ranks high because it can cause components to break prematurely and catastrophically with no obvious signs of impending collapse [50, 51, 52].
2	Uniform Corrosion	Mass transport, chemical reactions, interface involution, and electrochemical reactions at the metal/solution interface are some of the many intricate physical and electrochemical processes involved in uniform corrosion [55][56].
3	Pitting Corrosion	One kind of localized corrosion is pitting corrosion, which occurs when certain areas have a greater corrosion rate than others. Many alloys, although having a surface coating that protects them from general corrosion, can nonetheless experience pitting corrosion damage [57]–[59].
4	Intergranular Corrosion	Aggregate corrosion is a kind of corrosion in metal alloys caused by chemical interactions between individual metal grains [60][61].
5	Crevice Corrosion	When one metal surface comes into touch with the bulk electrolyte and another surface is exposed to the electrolyte that is trapped and stagnant in a "crevice," a specific kind of localized corrosion called crevice corrosion happens. Corrosion in metal crevices can be either passive, occurring at temperatures and potentials above critical, or non-passive, occurring in a non-specific environment due to active corrosion of the metal, or corrosion under deposits. Depassivation agents, primarily chloride, are used in the former case [39][46][47]. Oxygen transport into and metal ion diffusion out of are physically constrained [62]–[64].

Table 4. Corrosion Behavior 316L in Sea Water and Artificial Sea Water

No	Researcher	Method	Environment	Result
1.	Sabri Alkan, Mustafa Sabri Gok [65]	Scanning electron microscopy, energy-dispersive X-ray spectroscopy, potentiodynamics	Sea water	Pitting corrosion caused material losses of 0.00003 mm^3.
2	Daquan Li et al.[66]	Imaging techniques such as scanning electron microscopy, energy-dispersive x-ray spectroscopy, and immersion in environments with high pressure and temperature	Sea water	Corrosion rates in the material rose from 91% to 135% as a function of temperature and pressure; the phenomenon is known as stress corrosion.
3	W.M.K.M.W. Ihmal et al.[67]	Electrochemical impedance spectroscopy, scanning electron microscopy, Kalmegh coating, and potentiodynamic polarization	Sea water	At a concentration of 10% extract, the results demonstrated an improvement in corrosion resistance; however, the impact was concentration dependent, and higher increases reduced its inhibitory effect. Coated steel surfaces exhibited heterogeneous layers in SEM micrographs.
4	Haixian Liu et al.[23]	scanning electron microscopy, electrodynamic polarization, coating of extracellular polymeric substances (EPS),	Artificial sea water	The density of corrosion pits (>2 μm) reaches (5.6 ± 0.5) × 103 pits/cm^2 when the EPS concentration is 400 mg/L, and EPS speeds up both uniform and pitting corrosion.
5	Baoping Cai et al.[68]	Cyclic potentiodynamic polarization, scanning electron microscopy	Artificial sea water	crevice corrosion susceptibility with increasing applied torque

Table 5. Corrosion Behavior Inconel 600 in Sea Water and Artificial Sea Water

No	Researcher	Method	Environment	Result
1.	Van Rooyen D.[69]	Electron microscopy, potentiodynamic polarization	Sea water	The material experiences stress corrosion
2.	B Gregoire et al. [60]	Hot temperatur corrosion	Sea water	Molten chlorides cause pitting corrosion, which is a very destructive corrosion for materials.
3.	John H Heiser, Peter Soo [70]	Electron microscopy, potentiodynamic polarization	Sea water	The material experiences pitting corrosion
4.	M. prem kumar et al.[71]	Scanning electron microscopy, X-ray diffraction, and the hot immersion corrosion mechanism	Artificial water	The mass loss 0.002 g/cm^2
5.	Xian-Zong Wang et al.[72]	Tribocorrosion	Artificial water	Pitting corrosion and material loss can be detected by morphology detection on the material.

Direct contact with salt water can cause 316 stainless steel to develop holes if utilized for maritime purposes (marine enriched). The application of a specific coating on 316 stainless steel prevents pitting corrosion (avoiding direct contact with chlorides) [39].

Because of their particular preferences surface hardness, adhesive quality, long-term and high-temperature corrosion resistance, improved tribological characteristics, and so on coatings are useful for mitigating the effects of corrosive environments. Coatings can come in a range of thicknesses, from very thin to very thick, which opens up new possibilities for equipment design flexibility while cutting down on maintenance and machining expense [73].

A variety of methods exist for preventing corrosion, including coatings, cathodic protection, anodic protection, and inhibitors [74].

Coatings primarily serve to protect surfaces from corrosion, hence there is little emphasis on aesthetics and length resistance. Corrosive salts and air can easily penetrate damaged areas, but the coating must prevent them from penetrating the metal beneath. Coating thickness is often dictated by its intended application. Coatings that are intended to prevent air and corrosive salts from penetrating must be sufficiently thick to do so during their intended lifespan. For mechanically demanding applications, such as underground infrastructure, a thicker layer will provide better resistance [75].

One electrochemical method for limiting metal corrosion is cathodic protection. Metal buildings and equipment, whether subterranean, exposed to the elements, ship hulls, or heat exchangers, are protected against corrosion by the technique, which finds use in a wide range of industrial sectors around the globe. Globally and in a wide range of industries, to prevent the rusting and corrosion of metal components and parts used in a variety of applications, such as heat exchangers, ship hulls, underwater structures, and open marine constructions [76].

Anodic films with improved barrier layers, thicker film thickness, bigger pore cells, and broader pores are often the outcome of rising potential. Indeed, it has been discovered that the anodic film's formation voltage correlates with the layer thickness barrier, suggesting a relationship between carbon and hydrogen signals, in tartaric sulfuric acid [77].

Anode and ion refer to the metal that corrodes in the liquid. If the anode material has a passive surface in the electrolyte.

It can restrict the dissolution of the metal and the anode consumption rate, which is important because the metal enters into solution through the anodic oxidation reaction of anodic polarization. The four main components of an anodic protection system are the cathode, reference electrode, power supply, and potential controller. Anodic protection is commonly used to keep heat exchangers and other machinery that comes into contact with sulfuric acid from corroding [78].

To lessen the propensity for metal surfaces or surfaces exposed to corrosive fluids to corrode, corrosion inhibitors are tiny quantities of these compounds put to the surface. Common corrosion inhibitors, such chromium-based therapies, might be used with caution due to the fact that they are based on compounds that are dangerous to humans [79].

As an alternative, inhibitors can be used to manage the corrosion rate [80]. Some of the previous research on 316 stainless steel material application in corrosive environments with natural inhibitor are highlighted in the Table 6, for 316 stainless steel material application in corrosive environments with synthethic inhibitor are highlighted in the Table 7 and for 316 stainless steel material application in corrosive environments with coating are highlighted in the Table 8.

Table 9 shows some of the previous research on inconel 600 material application in corrosive environments with natural inhibitor, for inconel 600 material application in corrosive environments with synthethic inhibitor are highlighted in the Table 10 and for inconel 600 material application in corrosive environments with coating are highlighted in the Table 11.

Table 6. Natural Inhibitor in A316 Material

No.	Natural Inhibitor	Corrosive Environment	Reference
1	Date palm leaf extract	2% HCl Solution	[81]
2	Waste material (egg shell powder)	0.5 M H_2SO_4 Solution	[82]
3	Quinaldic acid (QDA), betaine (BET), dopamine hydrochloride (DOP), and diazolidinyl urea (DZU)	Sea water	.[83]
4	benzoic acid (C1), para-hydroxybenzoicacid (C2), and 3,4dihydroxybenzoic acid (C3)	HCl 0,5 M Solution	[84]
5	Arabic Gum	Acidic	[85]

Table 7. Synthetic Inhibitor in A316 Material

No.	Synthetic Inhibitor	Corrosive Environment	Reference
1	Monoehanolamine, chloroacetic acid, triethanolamine amine and vanillin	1,0 M HCl	.[86]
2	PPy-SMF NCs	NaCl 3,5%	[87]
3	Swertia chirata extract	Isotonic natural body fluids	[88]
4	PAni–SNF NCs	HCl 1,0 M	[89]
5	Thymus satureoides Oil	NaCl 3%	[90]
6	N-benzyl-N-(4-chlorophenyl)- 1H-tetrazole-5-amine	H_2SO_4	[91]

Table 8. Coating in A316 Material

No.	Coating	Corrosive Environment	Reference
1	Molybdenum Carbide Coating	HCl 1,0 M Solution	[92]
2	HA/f-MWCNT Coating	Stimulated body fluids	[93]
3	Superhydrofobic and oil coating	NaCl 3,5 %	[94]
4	Molybdenum disulfide	NaCl 3,5 %	[95]
5	Epoxy zinc oxide nanocomposite	NaCl 3,5 %	[96]
6	Ti6Al4V	NaCl 3,5 %	[97]

Table 9. Natural Inhibitor in Inconel 600 Material

No.	Natural Inhibitor	Corrosive Environment	Reference
1	Polyaspartic acid	0.04 M HCl	[98]
2	Rosmarinus officinalis	0.1 M HCl	[99]
3	Almond oil	0.01 M HCl	[100]
4	Natural clove oil	0.5 M HCl	[101]
5	Hydroxymethyl Aminomethane	0.2 M HCl	[102]

Table 10. Synthetic Inhibitor in Inconel 600 Material

No.	Synthetic Inhibitor	Corrosive Environment	Reference
1	Synthetic Fatty Acids	Chlorine	[103]
2	Molten-Salt Catalytic	Ternary Molten Chlorides	[103]
3	The synthesis of diamond	Methane-hydrogen chemical	[104]
4	Carbon nanotubes	1 M H_2SO_4	[105]
5	Silver-zinc Oxide	Ringer's solution	[106]

Table 11. Coating in Inconel 600 Material

No.	Coating	Corrosive Environment	Reference
1	Aluminide coatings	Na_2SO_4 solution	[107]
2	TiN	NaCl	[108]
3	Slurry Aluminade	NaCl	[109]
4	Cr_3C_2-NiCr	Salt Spray	[110]
5	Ni	Supercritical water	[111]

METHOD

An evaluation of the corrosion rate value of material 316 in a saltwater environment will typically be conducted as part of the research's qualitative technique.

Material

Create a 3-millimeter-thick material with dimensions of 2.5 by 2.5 centimeters [112]. Sanding and cleaning with abrasive paper 500, 800, and 1500 were among the pretreatment procedures used prior to the field exposure studies [113]. After that, it was washed with alcohol and distilled water [114].

Electrochemical Test

For the purpose of understanding how 316L corrosions, electrochemical tests were performed [115]. A potentiodynamic polarization test was performed using an electrochemical work station (CS-350) [116]. Electrolyte solutions were used for all corrosion experiments. The experiments used a three-electrode setup for electrochemical analysis [117].

Quicker results are obtained from electrochemical experiments compared to conventional laboratory tests. We can show the cathodic and anodic behavior of a metal in an environment with a wide range of oxidation and reduction potential in only a few minutes to a few hours thanks to our testing speeds that allow us to represent a complete polarization curve. In the technique, polarization is accomplished by controlling the current flowing through a corrosion cell, an electrical circuit that consists of an electrolyte and electrodes [118].

To monitor corrosion rates, estimate Tafel slopes, and observe the behavior of chemical processes, potentiostats are typically employed to generate potentiodynamic polarization curves, also known as Tafel curves. The gadget finds out how current flows through a metal's surface. There is now no complete knowledge of how temperature affects corrosion, but to acquaint the reader with the electrochemical impedance approach, it is briefly described. Here it is first presented. Two electrical ionic layers in the corrosion system provide a potential-based

electrical circuit between the test sample and the auxiliary electrode [119]

A silver/silver chloride (Ag/AgCl) reference electrode, a platinum (Pt) counter electrode, and the specimen itself serve as the electrodes for actual operations [120]. The impact of wear on corrosion can be better understood by corrosion wear testing. Prior to, during, and following corrosion wear, the open circuit potential fluctuation curves are seen. In order to produce a steady open circuit potential, potentiodynamic polarization measurements are performed. These measurements include taking the polarization curves of metal specimens under both corrosion-only and corrosion-wear situations [121].

Experimental settings used electrolytes made of STS 316L austenitic stainless steel in both saltwater and freshwater settings, as well as mixed water (seawater: freshwater = 1:1). In the aftermath of FR/VCP electro potential polarization studies, a Tafel analysis is performed. An electrode made of platinum (Pt) served as the counter electrode in the polarization experiment, while a reference electrode made of silver/silver chloride (Ag/Cl) was utilized. Soak in 30°C solution for 3,600 seconds before to conducting electrochemical polarization test. The open circuit potential after stabilization ranges from -0.25 V to 2.0 V relative to the open circuit potential, at a rate of 1.67 mV/s. Graph representing electro potential polarization Use Tafel extrapolation to determine Epit and Icorr, the corrosion current density. The potential for corrosion (Ecorr) is determined. Furthermore, subsequent to investigations using electrochemical polarization [120].

Table 12 shows some of the previous research electrochemical test on stainless steel 316 material, and Table 13 shows some of the previous research electrochemical test on Inconel 600.

Experiments on electrochemical polarization of STS 316L austenitic stainless steel in various environments, including fresh water, sea water, and mixed water, were conducted at a temperature of 30°C and shown in Figure 2. The creation of a passivation layer (Cr_2O_3) at the beginning of immersion causes the rise in current density to be relatively sluggish in the passivation part of the anode polarization curve. Unlike saltwater and mixed water, freshwater with the lowest Cl^-ion content exhibits a broad range of passivity and a rare pitting potential (Epit).

Table 12. Electrochemical Test 316L

No.	Researcher	Result	Type of Corrosion
1	Dana H Abdeen et al.[122]	The corrosion rate 0.0011 mm/yr and a current density of 0.1488 µA/cm^2	Pitting corrosion
2	P. Srisungsitthisunti and S.Mahathanabodee [123]	The corrosion rate 0.0017 mmpy	Pitting corrosion
3	N. R. Nik Masdek et al. [124]	The corrosion rate 0.0053 mmpy	Pitting corrosion
4	P. H. Setyarini et al.[125]	The corrosion rate 0.0148 mmpy	Pitting corrosion
5	P. Srisungsitthisunti et al.[126]	The corrosion rate 0.003 mm/yr	Pitting corrosion

Table 13. Electrochemical Test Inconel 600

No.	Researcher	Result	Type of Corrosion
1	J. T. Ho and G. P. Yu [127]	Both the anodic polarization scan and the open circuit immersion test yielded the same findings.	Pitting corrosion
2	W. Tsai et al.[128]	Test specimens made of INCONEL 600 alloy that had been subjected to potentials of -440 and +100 mV showed signs of pitting corrosion (SCE).	Pitting corrosion
3	K. Lyczkowska and J. Michalska [129]	The presence of heterogeneous dendrites or contaminants in the weld metal structure might be associated with spots where the corrosion process happens more quickly in Inconel 600 welds.	Pitting corrosion
4	E.-J. Jung and H.-W. Lee [130]	A passive film that is generally stable is demonstrated by the potentiodynamic polarization test. The possibility of pitting corrosion exists in Inconel 600.	Pitting corrosion
5	M. Abdallah et al [131]	The change in anodic volume and the corresponding values of the pitting potential are shifted to a more negative direction as a result of an increase in Cl^- content.	Pitting corrosion

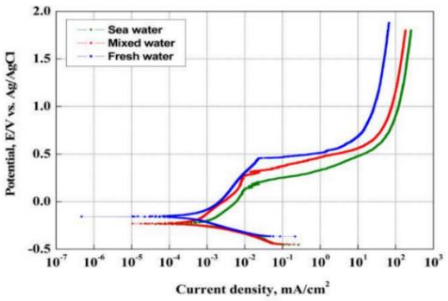

Figure 2. Potentiodynamic polarization curves of STS 316L in various solutions [120]

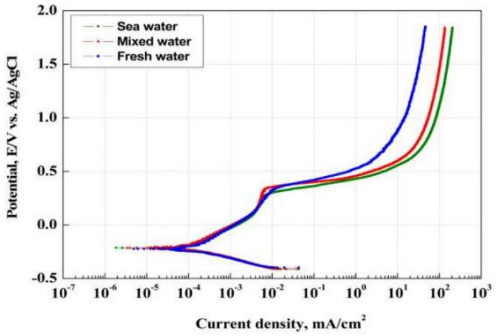

Figure 3. Potentiodynamic polarization curves of Inconel 600 in various solutions[120]

The value of Epit is a measure of resistance to the formula because it is derived from the potential formula, Epit. Officially, STS 316L has potentials of 0.139 V in saltwater, 0.271 V in mixed water, and 0.452 V in freshwater. In addition, the range of open circuit potential (OCP) to official Epit potential in saltwater is 0.375 V, in mixed water it is 0.502 V, and in freshwater it is 0.627 V. In saltwater, mixed water, and freshwater, the electromotive polarization experiment triggers the Cl^-ion active dissolving process; the leads to pitting as the oxide layer is destroyed, and the current density increases rapidly.

The formula involves substituting Cl^-ions with oxygen and hydroxyl groups in regions of the film where the passive structure is slightly unstable, causing damage to the film [132].

Seawater is Cl^-ion concentration is approximately 4.8 times greater than freshwater's, making the passive layer more susceptible to destruction. There are three distinct phases of hole development: nucleation, metastable, and stable. Additionally, the current density rises sharply in the presence of metastability holes. The metastability of STS 316L is shown to rise when the Cl^-concentration increases, as seen in the experimental data above [120].

According to studies, both the peak current intensity and the frequency of pit incidents are on the rise [133].

Inconel 600, a nickel alloy, was subjected to electro potential polarization studies in fresh water, salt water, and mixed water at 30^{o}C, as shown in Figure 3. Similar to STS 316L, a passivation section is seen at the point when the rise in current density comes to a halt, and a passive film (Cr_2O_3) is generated during the first immersion stage as a result of chromium [120].

In contrast to saltwater and mixed water, freshwater with the lowest Cl^-ion content exhibits a broad range of passivity and pitting potential (Epit).

Inconel 600, in contrast to STS 316L, has a narrower range of pitting potential and passivity sections determined by the measured solution factors. In line with the findings of salt-dependent corrosion studies conducted on Inconel 600, STS 304, Incoloy, and STS 316 in the nearby area [30].

Compared to the nickel alloy, the change in pitting potential as a function of the NaCl concentration between STS 304 and STS 316 was much larger. In saltwater, mixed water, and freshwater, the official potential of Inconel 600 was found to be 0.301 V, 0.335 V, and 0.343 V, respectively. Additionally, in saltwater, mixed water, and freshwater, the range of open circuit potential (OCP) to official Epit potential is 0.563 V, 0.551 V, and 0.515 V, respectively. When the active dissolving process of Cl^-ions became active, the oxide layer broke down, leading to the rapid rise in current density seen in the electro potential polarization tests [120].

Figure 4 displays the outcomes of the Tafel and polarization curve analyses performed on STS 316L and Inconel 600 after the electropotential polarization experiment. For STS 316L, the corrosion current densities are 7.75 × 10-4, 4.13 × 10-4, and 2.85, correspondingly. According to the order of × 10^-4 mA/cm², sea water has the greatest electrical conductivity and a large concentration of Cl_2 ions, which significantly affects the frequency of corrosion, compared to mixed water and fresh water, which have lower ion concentrations.

Based on the findings of the electromotive polarization experiment, it was observed that as the concentration of Cl^-increasing, the corrosion current density rises and the pitting potential and corrosion potential shift towards the non-dislocation direction. When examining surface damage, pitting damage may happen in saltwater.

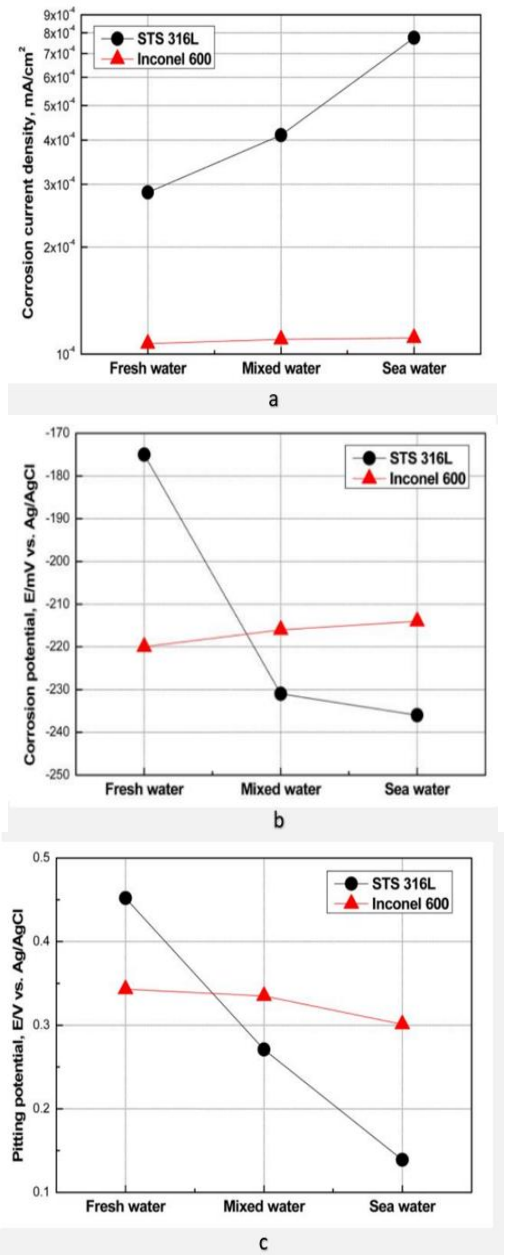

Figure 4. Results of polarization curve analysis and Tafel analysis after potentiodynamic experiments on various solutions. a. Corrosion Current Density b. Corrosion Potential c. Pitting Potential[120]

Meanwhile, in sea water, mixed water, and fresh water, the corrosion current density of Inconel 600 is 1.11 × 10-4 mA/cm², 1.10 × 10⁴, and 1.07 × 10⁴ mA/cm², respectively. The corrosion current density difference between Inconel 600 and STS 316L, as determined by solution variables, is much less for Inconel 600. Complete corrosion rate may be calculated by plugging the corrosion current density into the Faraday equation. Table 14 shows the chemical composition stainless steel 316 material and inconel 600 material.

SEM (Scanning Electron Microscope)

The following is an image of surface morphology taken from a microscope. Figure 5 is the surface shape observed with a scanning electron microscope after electro potential polarization experiments. In both specimens, with increasing Cl^- concentration, size and number of pitting holes increase. This is in accordance with the results of surface scanning. From the results of this experiment, it can be seen that Inconel 600 experiences less corrosion damage in neutral chloride solutions compared to STS 316L which has a relatively high PREN index.

Table 14. Chemical Compositions of 316L and Inconel 600 [120]

	C	Si	Mn	P	S	Cr	Ni	Mo	Cu	N	Al	Fe
316 L	0.023	0.603	1.05	0.034	0.003	16.7	10.19	2.03	0.282	0.012	0.003	Bal
Inconel 600	0.05	0.24	0.33	-	0.006	15.7	73.7	-	0.03	-	-	8.8

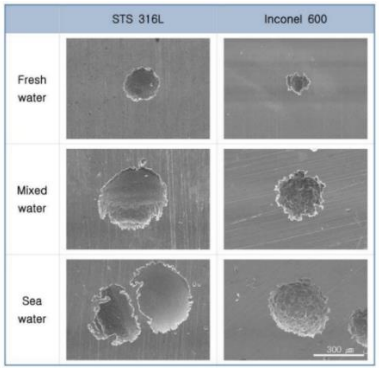

Figure 5. Surface morphology after potentiodynamic polarization experiments of STS 316L and Inconel 600 in various solutions [120]

In other words, it seems difficult to compare the pitting resistance of Fe-based alloys and Ni-based alloys with the same ÿ-austenite phase structure using simple PREN values [120].

In line with what surface scanning revealed. The experiment's findings show that, in neutral chloride solutions, Inconel 600 is less susceptible to corrosion than STS 316L, a material with a higher PREN index. Put differently, it seems to be challenging to use basic PREN values to compare the pitting resistance of Fe-based alloys with Ni-based alloys with the same y-austenite phase structure.

In order for corrosion to take place, an anodic reaction must take place between iron and nickel. The electro potential polarization test revealed that every specimen had substantial pitting damage. The proves that without cathodic protection and coating, using STS 316L or Inconel 600 in a maritime setting is rather challenging.

Standards for material selection in maritime and petrochemical settings, such as NORSOK M-001 and ISO 21457, state that cathodic protection is required for materials with a PREN value below 40 [133].

CONCLUSION

Corrosion studies on 316 pipes in salt water conditions are reviewed, along with the different forms of corrosion, inhibitors, and methods for assessing corrosion rates (electrochemical and scanning electron microscopy).

Alterations to the concentration of saltwater allowed the electrochemical process to produce the nickel alloy Inconel 600 and the austenitic stainless steel STS 316L. The Tafel analysis revealed that all specimens contained either salt water, mixed water, or fresh water.

An elevated value is displayed by the corrosion current density. Corrosion current density variations in Inconel 600 with respect to solution parameters are substantially less than those in STS 316L.

Although Inconel 600 has a lower pitting resistance index than STS 316L, the latter is shown to do more damage in any given solution when pitting corrosion is a concern. Put simply, comparing the pitting resistance of stainless steel based on iron and Inconel based on nickel is not an easy task.

Because chlorine speeds up the corrosion process, alloys like Inconel 600 and 316L both undergo pitting corrosion. According to what was said earlier, the molybdenum concentration in 316 stainless steel gives it better corrosion resistance. that's why it works well for gas and oil pipelines that go through saltwater. Nevertheless, materials exposed to maritime environments must have cathodic protection or coating put to them in order to prolong their life and stop the pipe from continuously corroding.

In previous research conducted by Senka Gudic et al. [134][135] using AISI 304L and AISI 316L materials in seawater with open circuit potential measurements, linear and potentiodynamic polarization, and electrochemical impedance spectroscopy. It was found that increasing temperature and pollutant concentrations have a negative impact on the corrosion stability of stainless steel in open circuits. The occurrence of pitting corrosion on the surface of the samples was confirmed by an optical microscope and a non-contact 3D profilometer. With increasing temperature and sulfide ion concentration, the width, depth and density of pitting in both steel samples increased.

BIBLIOGRAPHY

[1] Y. Shigetomi, Y. Ishimura, and Y. Yamamoto, “Trends in global dependency on the Indonesian palm oil and resultant environmental impacts,” *Sci. Rep.*, vol. 10, no. 1, p. 20624, 2020, doi: 10.1038/s41598-020-77458-4.

[2] R. Syahrir, F. Wall, and P. Diallo, “Socio-economic impacts and sustainability of mining, a case study of the historical tin mining in Singkep Island-Indonesia,” *Extr. Ind. Soc.*, vol. 7, no. 4, pp. 1525–1533, 2020, doi: https://doi.org/10.1016/j.exis.2020.07.023.

[3] A. Rahman, P. Dargusch, and D. Wadley, “The political economy of oil supply in Indonesia and the implications for renewable energy development,” *Renew. Sustain. Energy Rev.*, vol. 144, no. April, p. 111027, 2021, doi: 10.1016/j.rser.2021.111027.

[4] O. Agboola *et al.*, “Results in Engineering A review on the impact of mining operation : Monitoring , assessment and management,” *Results Eng.*, vol. 8, no. July, p. 100181, 2020, doi: 10.1016/j.rineng.2020.100181.

[5] Y. Liu *et al.*, “A review of treatment technologies for produced water in offshore oil and gas fields,” *Sci. Total Environ.*, vol. 775, p. 145485, 2021, doi: https://doi.org/10.1016/j.scitotenv.2021.145485.

[6] S. Razvarz, R. Jafari, and A. Gegov, “Flow modelling and control in pipeline systems,” *Stud. Syst. Decis. Control*, vol. 321, no. 1, pp. 25–57, 2021, doi: 10.1007/978-3-030-59246-2.

[7] A. M. Rahmani, S. Ali, M. H. Malik, and E. Yousefpoor, “An energy - aware and Q - learning - based area coverage for oil pipeline monitoring systems using sensors and Internet of Things,” *Sci. Rep.*, pp. 1–17, 2022, doi: 10.1038/s41598-022-12181-w.

[8] K. Fang, C. Li, S. Dong, D. Zhang, X. Wu, and H. Hu, “Effect of Cu2+ on Corrosion Behavior of A106B Carbon Steel and 304L Stainless Steels in Seawater,” *Scanning*, vol. 2021, no. 1–10, p. 6661872, 2021, doi: 10.1155/2021/6661872.

[9] D. Kalaimani and G. Srinivasan, “Strength and durability properties of concrete made with recycled coarse aggregate and seashore sand,” *SINERGI*, vol. 28, no. 1, pp. 115–128, 2024, doi: 10.22441/sinergi.2024.1.012.

[10] V. U. Elechi, S. S. Ikiensikimama, O. E. Akaranta, J. A. Ajienka, M. O. Onyekonwu, and O. E. Okon, “The use of a bench-scale high pressure apparatus to evaluate the effectiveness of a locally sourced material as gas hydrate inhibitor,” *Sci. African*, vol. 8, p. e00300, 2020, doi: 10.1016/j.sciaf.2020.e00300.

[11] H. Li *et al.*, “Corrosion crack failure analysis of 316L hydraulic control pipeline in high temperature aerobic steam environment of heavy oil thermal recovery well,” *Eng. Fail. Anal.*, vol. 138, p. 106297, 2022, doi: 10.1016/j.engfailanal.2022.106297.

[12] F. Ostovan, E. Shafiei, M. Toozandehjani, I. F. Mohamed, and M. Soltani, “On the role of molybdenum on the microstructural, mechanical and corrosion properties of the GTAW AISI 316 stainless steel welds,” *J. Mater. Res. Technol.*, vol. 13, pp. 2115–2125, 2021, doi: 10.1016/j.jmrt.2021.05.095.

[13] Y.-T. Sun, X. Tan, L.-L. Lei, J. Li, and Y.-M. Jiang, “Revisiting the effect of molybdenum on pitting resistance of stainless steels,” *Tungsten*, vol. 3, no. 3, pp. 329–337, 2021, doi: 10.1007/s42864-021-00099-1.

[14] A. Di Schino and C. Testani, “Corrosion Behavior and Mechanical Properties of AISI 316 Stainless Steel Clad Q235 Plate,” *Metals*, vol. 10, no. 4. 2020. doi: 10.3390/met10040552.

[15] F. S. da Luz, W. A. Pinheiro, S. N. Monteiro, V. S. Candido, and A. C. R. da Silva, “Mechanical properties and microstructural characterization of a novel 316L austenitic stainless steel coating on A516 Grade 70 carbon steel weld,” *J. Mater. Res. Technol.*, vol. 9, no. 1, pp. 636–640, 2020, doi: 10.1016/j.jmrt.2019.11.004.

[16] S. Yan, Y. Shi, J. Liu, and C. Ni, “Effect of laser mode on microstructure and corrosion resistance of 316L stainless steel weld joint,” *Opt. Laser Technol.*, vol. 113, pp. 428–436, 2019, doi: 10.1016/j.optlastec.2019.01.023.

[17] S. Akbar, D. Nursyifaulkhair, L. Nurdiwijayanto, A. Noviyanto, and N. T. Rochman, “High-temperature failure of steel boiler tube secondary superheater in a power plant,” *SINERGI*, vol. 27, no. 1, pp. 1–6, 2023, doi: 10.22441/sinergi.2023.1.001.

[18] M. Yazdi, F. Khan, R. Abbassi, N. Quddus, and H. Castaneda-Lopez, “A review of risk-based decision-making models for microbiologically influenced corrosion (MIC) in offshore pipelines,” *Reliab. Eng. Syst. Saf.*, vol. 223, p. 108474, 2022, doi: https://doi.org/10.1016/j.ress.2022.108474.

[19] S. Pahlavan, M. H. Moayed, and M. Mirjalili, "The Contrast between the Pitting Corrosion of 316 SS in NaCl and NaBr Solutions: Part I. Evolution of Metastable Pitting and Stable Pitting," *J. Electrochem. Soc.*, vol. 166, no. 2, p. C65, 2019, doi: 10.1149/2.0811902jes.

[20] H. Tian *et al.*, "Effect of NH4+ on the pitting corrosion behavior of 316 stainless steel in the chloride environment," *J. Electroanal. Chem.*, vol. 894, p. 115368, 2021, doi: 10.1016/j.jelechem.2021.115368.

[21] L. Guo *et al.*, "Effect of Mixed Salts on Atmospheric Corrosion of 304 Stainless Steel," *J. Electrochem. Soc.*, vol. 166, no. 11, p. C3010, 2019, doi: 10.1149/2.0021911jes.

[22] S. Pal, S. S. Bhadauria, and P. Kumar, "Pitting Corrosion Behavior of F304 Stainless Steel Under the Exposure of Ferric Chloride Solution," *J. Bio- Tribo-Corrosion*, vol. 5, no. 4, p. 91, 2019, doi: 10.1007/s40735-019-0283-z.

[23] H. Liu, J. He, Z. Jin, and H. Liu, "Pitting corrosion behavior and mechanism of 316L stainless steel induced by marine fungal extracellular polymeric substances," *Corros. Sci.*, vol. 224, p. 111485, 2023, doi: 10.1016/j.corsci.2023.111485.

[24] M. M. Prabhakar *et al.*, "An overview of burst , buckling , durability and corrosion analysis of lightweight FRP composite pipes and their applicability a Department," *Compos. Struct.*, p. 111419, 2019, doi: 10.1016/j.compstruct.2019.111419.

[25] I. G. A. Arwati, N. Euis, and D. Sirait, "Cathodic Protection in Onshore Pipe Networks Gas Pagardewa Receiving Station," *World Chem. Eng. J.*, vol. 3, no. 1, pp. 24–29, 2019, doi: 10.36055/wcej.v3i1.5613.

[26] Z. Tang, "a review of corrosion inhibitors for rust preventative fluids," *Curr. Opin. Solid State Mater. Sci.*, vol. 23(4), no. February, pp. 1–16, 2019, doi: 10.1016/j.cossms.2019.06.003.

[27] Q. Zhu, B. Zhang, M. Zheng, X. Zhao, and J. Xu, "Corrosion Behaviors of S355 Steel under Simulated Tropical Marine Atmosphere Conditions," *J. Mater. Eng. Perform.*, vol. 31, no. 12, pp. 10054–10062, 2022, doi: 10.1007/s11665-022-07041-7.

[28] E. M. Costa, B. A. Dedavid, C. A. Santos, C. Fraccaro, T. Pagartanidis, and L. P. Lovatto, "Crevice corrosion on stainless steels in oil and gas industry : A review of techniques for evaluation , critical environmental factors and dissolved oxygen," vol. 144, no. July 2022, 2023, doi: 10.1016/j.engfailanal.2022.106955.

[29] C. Kim, L. Chen, H. Wang, and H. Castaneda, "Global and local parameters for characterizing and modeling external corrosion in underground coated steel pipelines: A review of critical factors," *J. Pipeline Sci. Eng.*, vol. 1, no. 1, pp. 17–35, 2021, doi: https://doi.org/10.1016/j.jpse.2021.01.010.

[30] A. R. Prasad, A. Kunyankandy, A. Joseph, and A. J. Munzer, "Corrosion Inhibition in Oil and Gas Industry : Economic Considerations," *Corros. Inhib. Oil Gas Ind.*, pp. 135–150, 2020, doi: 10.1002/9783527822140.ch5.

[31] H. M. Ezuber, A. Alshater, S. M. Z. Hossain, and A. El-Basir, "Impact of Soil Characteristics and Moisture Content on the Corrosion of Underground Steel Pipelines," *Arab. J. Sci. Eng.*, vol. 46, no. 7, pp. 6177–6188, 2021, doi: 10.1007/s13369-020-04887-8.

[32] W. G. Bell, S., Steinberg, T, "Corrosion mechanisms in molten salt thermal energy storage for concentrating solar power," *Elsevier*, vol. 114, p. 1093281, 2019, doi: doi.org/10.1016/j.rser.2019.109328.

[33] B. J. Little *et al.*, "Microbially influenced corrosion-Any progress?," *Corros. Sci.*, vol. 170, no. November 2019, p. 108641, 2020, doi: 10.1016/j.corsci.2020.108641.

[34] K. Lakkam, S. Mkerur, and A. Shirahatti, "Effect of pitting corrosion on the mechanical properties of 316 grade stainless steel," *Mater. Today Proc.*, vol. 27, no. 1, pp. 497–502, 2020, doi: 10.1016/j.matpr.2019.11.293.

[35] K. V Akpanyung and R. T. Loto, "Pitting corrosion evaluation: a review," in *Journal of Physics: Conference Series*, 2019, vol. 1378, no. 2, p. 22088. doi: 10.1088/1742-6596/1378/2/022088.

[36] S. Jafarzadeh, Z. Chen, and F. Bobaru, "Computational modeling of pitting corrosion," *Corros. Rev.*, vol. 37, no. 5, pp. 419–439, 2019, doi: 10.1515/corrrev-2019-0049.

[37] Y. Zhao, X. Xu, Y. Wang, and J. Dong, "Characteristics of pitting corrosion in an existing reinforced concrete beam exposed to marine environment," *Constr. Build. Mater.*, vol. 234, p. 117392, 2020, doi: 10.1016/j.conbuildmat.2019.117392.

[38] B. Zhang and X. L. Ma, "Journal of Materials Science & Technology A review — Pitting corrosion initiation investigated by TEM," *Elsevier*, vol. 35, pp. 1455–1465, 2019, doi:

10.1016/j.jmst.2019.01.013.
[39] S. T. Kumaran and K. Baranidharan, “Corrosion Studies on Stainless Steel 316 and their Prevention – A Review,” *Incas Bull.*, vol. 13, no. 3, pp. 245–251, 2021, doi: 10.13111/2066-8201.2021.13.3.21.
[40] Y. Gao, Y. Zheng, J. Zhang, S. Xu, X. Zhou, and Y. Zhang, “Time-dependent corrosion process and non-uniform corrosion of reinforcement in RC flexural members in a tidal environment,” *Constr. Build. Mater.*, vol. 213, pp. 79–90, 2019, doi: 10.1016/j.conbuildmat.2019.04.088.
[41] Y. Blikharskyy, N. Kopiika, and J. Selejdak, “Non-uniform corrosion of steel rebar and its influence on reinforced concrete elements reliability,” *Prod. Eng. Arch.*, vol. 26, no. 2, pp. 67–72, 2020, doi: 10.30657/pea.2020.26.14.
[42] C. Shi, Y. Gong, Z. Yang, and Q. Tong, “Peridynamic investigation of stress corrosion cracking in carbon steel pipes,” *Eng. Fract. Mech.*, vol. 219, no. April, p. 106604, 2019, doi: 10.1016/j.engfracmech.2019.106604.
[43] A. R. Khasanova, “Stress corrosion cracking in pipelines,” *Mater. Sci. Eng.*, vol. 952, no. 1, p. 012046, 2020, doi: 10.1088/1757-899X/952/1/012046.
[44] Y. Lv *et al.*, “Materials Characterization Investigation of microscopic residual stress and its effects on stress corrosion behavior of NiAl bronze alloy using in situ neutron diffraction / EBSD / tensile corrosion experiment,” *Mater. Charact.*, vol. 164, no. April, p. 110351, 2020, doi: 10.1016/j.matchar.2020.110351.
[45] J. Zhao, S. Jafarzadeh, M. Rahmani, Z. Chen, Y. Kim, and F. Bobaru, “Electrochimica Acta A peridynamic model for galvanic corrosion and fracture,” vol. 391, 2021, doi: 10.1016/j.electacta.2021.138968.
[46] W. Xu, B. Zhang, O. Addison, X. Wang, B. Hou, and F. Yu, “Mechanically-assisted crevice corrosion and its effect on materials degradation,” *Corros. Commun.*, vol. 11, pp. 23–32, 2023, doi: 10.1016/j.corcom.2023.01.002.
[47] S. Jafarzadeh, J. Zhao, M. Shakouri, and F. Bobaru, “A peridynamic model for crevice corrosion damage,” *Electrochim. Acta*, vol. 401, p. 139512, 2022, doi: 10.1016/j.electacta.2021.139512.
[48] H. Wu *et al.*, “Crevice Corrosion – A Newly Observed Mechanism of Degradation in Biomedical Magnesium,” *Acta Biomater.*, 2019, doi: 10.1016/j.actbio.2019.06.013.
[49] Q. B. Nguyen *et al.*, “The role of abrasive particle size on erosion characteristics of stainless steel,” *Eng. Fail. Anal.*, vol. 97, pp. 844–853, 2019, doi: https://doi.org/10.1016/j.engfailanal.2019.01.020.
[50] R. J. Chung, J. Jiang, C. Pang, B. Yu, R. Eadie, and D. Y. Li, “Erosion-corrosion behaviour of steels used in slurry pipelines,” no. September 2020, 2021, doi: 10.1016/j.wear.2021.203771.
[51] Y. Xu, L. Liu, Q. Zhou, X. Wang, and Y. Huang, “Understanding the influences of pre-corrosion on the erosion-corrosion performance of pipeline steel,” *Wear*, p. 203151, 2020, doi: 10.1016/j.wear.2019.203151.
[52] M. A. Kappes, “Localized corrosion and stress corrosion cracking of stainless steels in halides other than chlorides solutions: a review,” vol. 38, no. 1, pp. 1–24, 2020, doi: 10.1515/corrrev-2019-0061.
[53] T. M. Ahn, “Long-term initiation time for stress -corrosion cracking of alloy 600 with implications in stainless steel: Review and analysis for nuclear application,” *Prog. Nucl. Energy*, vol. 137, p. 103760, 2021, doi: 10.1016/j.pnucene.2021.103760.
[54] L. Calabrese and E. Proverbio, “A Review on the Applications of Acoustic Emission Technique in the Study of Stress Corrosion Cracking,” *Corrosion and Materials Degradation*, vol. 2, no. 1. pp. 1–30, 2021. doi: 10.3390/cmd2010001.
[55] K. Wang, C. Li, Y. Li, J. Lu, Y. Wang, and X. Luo, “A fully coupled model of hydrodynamic-chemical-electrochemical processes for CO2 uniform corrosion in multi-physics environment,” *J. Pet. Sci. Eng.*, vol. 193, p. 107436, 2020, doi: 10.1016/j.petrol.2020.107436.
[56] K.-S. Lim, W.-S. Choi, W.-B. Kim, S.-H. Cho, and J.-H. Lee, “Effect of Cr Content on Hot Corrosion Behavior of Inconel Alloys in Molten LiCl–Li2O,” *High Temp. Corros. Mater.*, vol. 100, no. 3, pp. 345–358, 2023, doi: 10.1007/s11085-023-10180-4.
[57] S. Jafarzadeh, Z. Chen, and F. Bobaru, “Computational modeling of pitting corrosion,” vol. 37, no. 5, pp. 419–439, 2019, doi: 10.1515/corrrev-2019-0049.
[58] B. Grégoire, C. Oskay, T. M. Meißner, and M. C. Galetz, “Corrosion mechanisms of ferritic-martensitic P91 steel and Inconel 600 nickel-based alloy in molten chlorides. Part I: NaCl–KCl binary system,” *Sol. Energy Mater. Sol. Cells*, vol. 215, p. 110659, 2020, doi:

10.1016/j.solmat.2020.110659.
[59] C. Guo, S. Shi, H. Dai, J. Yu, and X. Chen, "Corrosion mechanisms of nickel-based alloys in chloride-containing hydrofluoric acid solution," *Eng. Fail. Anal.*, vol. 140, p. 106580, 2022, doi: 10.1016/j.engfailanal.2022.106580.
[60] B. Grégoire, C. Oskay, T. M. Meißner, and M. C. Galetz, "Corrosion mechanisms of ferritic-martensitic P91 steel and Inconel 600 nickel-based alloy in molten chlorides. Part II: NaCl-KCl-MgCl2 ternary system," *Sol. Energy Mater. Sol. Cells*, vol. 216, p. 110675, 2020, doi: 10.1016/j.solmat.2020.110675.
[61] L. Volpe, G. Bertali, F. Scenini, and M. G. Burke, "Effect of temperature on the preferential intergranular oxidation susceptibility of thermally-treated Alloy 600," *Corros. Sci.*, vol. 207, p. 110565, 2022, doi: 10.1016/j.corsci.2022.110565.
[62] F. Ning *et al.*, "Nodular corrosion inside the crevice of Alloy 690 in deaerated high-temperature chloride solution," *Corros. Sci.*, vol. 185, p. 109442, 2021, doi: 10.1016/j.corsci.2021.109442.
[63] W. Xu, B. Zhang, O. Addison, X. Wang, and B. Hou, "Mechanically-assisted crevice corrosion and its effect on materials degradation," *Corros. Commun.*, vol. 11, pp. 23–32, 2023, doi: 10.1016/j.corcom.2023.01.002.
[64] F. Ning, X. Wu, and J. Tan, "Crevice corrosion behavior of Alloy 690 in high-temperature water," *J. Nucl. Mater.*, vol. 515, pp. 326–337, 2019, doi: 10.1016/j.jnucmat.2018.12.050.
[65] S. Alkan and M. S. Gök, "Effect of sliding wear and electrochemical potential on tribocorrosion behaviour of AISI 316 stainless steel in seawater," *Eng. Sci. Technol. an Int. J.*, vol. 24, no. 2, pp. 524–532, 2021, doi: 10.1016/j.jestch.2020.07.004.
[66] D. Li, Q. Liu, W. Wang, L. Jin, and H. Xiao, "Corrosion Behavior of AISI 316L Stainless Steel Used as Inner Lining of Bimetallic Pipe in a Seawater Environment," *Materials (Basel).*, vol. 14, no. 6, 2021, doi: 10.3390/ma14061539.
[67] W. Ikhmal *et al.*, "Evaluating the performance of andrographis paniculata leaves extract as additive for corrosion protection of stainless steel 316l in seawater," *Int. J. Corros. Scale Inhib.*, vol. 9, no. 1, pp. 118–133, 2020, doi: 10.17675/2305-6894-2020-9-1-7.
[68] B. Cai, Y. Liu, X. Tian, F. Wang, H. Li, and R. Ji, "An experimental study of crevice corrosion behaviour of 316L stainless steel in artificial seawater," *Corros. Sci.*, vol. 52, no. 10, pp. 3235–3242, 2010, doi: 10.1016/j.corsci.2010.05.040.
[69] D. Van Rooyen, "Review of the Stress Corrosion Cracking of Inconel 600," *Corrosion*, vol. 31, no. 9, pp. 327–337, Jan. 2013, doi: 10.5006/0010-9312-31.9.327.
[70] J. H. Heiser and P. Soo, "Corrosion of barrier materials in seawater environments," United States, 1995. [Online]. Available: http://inis.iaea.org/search/search.aspx?orig_q=RN:27032332
[71] M. Prem Kumar, N. Arivazhagan, C. Chiranjeevi, Y. Raja Sekhar, N. Babu, and M. Manikandan, "Effect of Molten Binary Salt on Inconel 600 and Hastelloy C-276 Superalloys for Thermal Energy Storage Systems: A Corrosion Study," *J. Mater. Eng. Perform.*, 2023, doi: 10.1007/s11665-023-08641-7.
[72] X.-Z. Wang, Y. Wang, Z. Huang, Q. Zhou, and H. Wang, "Tribocorrosion Behavior of CoCrNi Medium Entropy Alloy in Simulated Seawater," *Metals*, vol. 12, no. 3. 2022. doi: 10.3390/met12030401.
[73] A. A. Farag, "Applications of nanomaterials in corrosion protection coatings and inhibitors," no. June, 2023, doi: 10.1515/corrrev-2019-0011.
[74] S. K. Dhawan, H. Bhandari, G. Ruhi, B. Mohan, S. Bisht, and P. Sambyal, *Corrosion Preventive Materials and Corrosion Testing*, no. May. CRC Press, 2020. doi: 10.1201/9781315101217.
[75] S. G. Croll, "Surface roughness profile and its effect on coating adhesion and corrosion protection: A review," *Prog. Org. Coatings*, vol. 148, p. 105847, 2020, doi: 10.1016/j.porgcoat.2020.105847.
[76] U. M. Angst, "A Critical Review of the Science and Engineering of Cathodic Protection of Steel in Soil and Concrete," vol. 75, no. 12, pp. 1420–1433, 2019, doi: 10.5006/3355.
[77] M. Paz Martínez-Viademonte, S. T. Abrahami, T. Hack, M. Burchardt, and H. Terryn, "A review on anodizing of aerospace aluminum alloys for corrosion protection," *Coatings*, vol. 10, no. 11, p. 1106, 2020, doi: 10.3390/coatings10111106.
[78] W. Faes *et al.*, "Corrosion and corrosion prevention in heat exchangers," *Corros. Rev.*, vol. 37, no. 2, pp. 131–155, 2019, doi: 10.1515/corrrev-2018-0054.

[79] D. Puthran and D. Patil, “Usage of heavy metal-free compounds in surface coatings,” *J. Coatings Technol. Res.*, vol. 20, no. 1, pp. 87–112, 2023, doi: 10.1007/s11998-022-00648-4.

[80] Z. Feng, C. Liu, and S. Schippers, “Economic Impact of Corrosion in Oil Sectors and Prevention : An Overview Economic Impact of Corrosion in Oil Sectors and Prevention : An Overview,” 2019, doi: 10.1088/1742-6596/1378/2/022037.

[81] I. B. Obot *et al.*, “Development of a green corrosion inhibitor for use in acid cleaning of MSF desalination plant,” *Desalination*, vol. 495, no. June, p. 114675, 2020, doi: 10.1016/j.desal.2020.114675.

[82] O. F. , O Sanni, API Popoola, “Temperature Effect , Activation Energies and Adsorption Studies of Waste Temperature Effect , Activation Energies and Adsorption Studies of Waste Material as Stainless Steel Corrosion Inhibitor in Sulphuric,” *J. Bio-Tribo-Corrosion*, no. October, pp. 0–8, 2019, doi: 10.1007/s40735-019-0280-2.

[83] T. N. Myasoedova, R. Kalusulingam, and T. S. Mikhailova, “Sol-Gel Materials for Electrochemical Applications: Recent Advances,” *Coatings*, vol. 12, no. 11, p. 1625, 2022, doi: 10.3390/coatings12111625.

[84] M. Alahiane *et al.*, “Electrochemical , thermodynamic and molecular dynamics studies of some benzoic acid derivatives on the corrosion inhibition of 316 stainless steel in HCl solutions,” vol. 328, 2021, doi: 10.1016/j.molliq.2021.115413.

[85] I. Arwati *et al.*, “Effect of Arabic Gum Electrophoresis Desposition on Corrosion of SS316L in Acidic,” *J. Kejuruter.*, vol. 1, no. 1, pp. 59–64, 2018, doi: 10.17576/jkukm-2018-si1(1)-08.

[86] S. M. Shaban, S. Abd Elsamad, S. M. Tawfik, A.-H. Adel, and I. Aiad, “Studying surface and thermodynamic behavior of a new multi-hydroxyl Gemini cationic surfactant and investigating their performance as corrosion inhibitor and biocide,” *J. Mol. Liq.*, vol. 316, p. 113881, 2020, doi: 10.1016/j.molliq.2020.113881.

[87] P. Muthusamy, “High efficient corrosion inhibitor of water-soluble polypyrrole – sulfonated melamine formaldehyde nanocomposites for 316 L stainless steel,” no. May, pp. 1–14, 2020, doi: 10.1002/app.49952.

[88] P. Sharma, N. Bhardwaj, and V. Kumar, “Swertia chirata extract mediated synthesis of iron oxide nanoparticles and its use as corrosion inhibitor for stainless steel 316 L in Ringer’s solution,” *Adv. Nat. Sci. Nanosci. Nanotechnol.*, vol. 12, no. 3, p. 35012, 2021, doi: 10.1088/2043-6262/ac2742.

[89] M. Packiaraj and K. K. S. Kumar, “High corrosion protective behavior of water-soluble conducting polyaniline–sulfonated naphthalene formaldehyde nanocomposites on 316L SS,” *J. Alloys Compd.*, vol. 864, p. 158345, 2021, doi: 10.1016/j.jallcom.2020.158345.

[90] F. Simescu-Lazar *et al.*, “Thymus satureoides Oil as Green Corrosion Inhibitor for 316L Stainless Steel in 3% NaCl: Experimental and Theoretical Studies,” *Lubricants*, vol. 11, no. 2. 2023. doi: 10.3390/lubricants11020056.

[91] M. A. Fajobi, R. T. Loto, and O. O. Oluwole, “Austenitic 316L stainless steel; corrosion and organic inhibitor: a review,” *Key Eng. Mater.*, vol. 886, pp. 126–132, 2021, doi: 10.4028/www.scientific.net/kem.886.126.

[92] L. Wang *et al.*, “ScienceDirect Molybdenum carbide coated 316L stainless steel for bipolar plates of proton exchange membrane fuel cells,” *Int. J. Hydrogen Energy*, 2019, doi: 10.1016/j.ijhydene.2018.12.184.

[93] D. Sivaraj and K. Vijayalakshmi, “Ultrasonics - Sonochemistry Enhanced antibacterial and corrosion resistance properties of Ag substituted hydroxyapatite / functionalized multiwall carbon nanotube nanocomposite coating on 316L stainless steel for biomedical application,” *Ultrason. - Sonochemistry*, vol. 59, no. July, p. 104730, 2019, doi: 10.1016/j.ultsonch.2019.104730.

[94] Z. Yang, X. Liu, and Y. Tian, “Progress in Organic Coatings A contrastive investigation on anticorrosive performance of laser-induced super-hydrophobic and oil-infused slippery coatings,” *Prog. Org. Coatings*, vol. 138, no. June 2019, p. 105313, 2020, doi: 10.1016/j.porgcoat.2019.105313.

[95] M.-S. Hong, Y. Park, J. G. Kim, and K. Kim, “Effect of Incorporating MoS2 in Organic Coatings on the Corrosion Resistance of 316L Stainless Steel in a 3.5% NaCl Solution,” *Coatings*, vol. 9, no. 1. 2019. doi: 10.3390/coatings9010045.

[96] N. F. Ibrahim, W. R. Wan Abdullah, M. S. Rooshde, M. S. Mohd Ghazali, and W. B. Wan Nik, “Corrosion inhibition properties of epoxy-zinc oxide nanocomposite coating on stainless steel 316L,” *Solid State Phenom.*,

vol. 307, pp. 285–290, 2020, doi: 10.4028/www.scientific.net/ssp.307.285.
[97] R. Yamanoglu, E. Fazakas, F. Ahnia, D. Alontseva, and F. Khoshnaw, “Pitting corrosion behaviour of austenitic stainless-steel coated on Ti6Al4V alloy in chloride solutions,” *Adv. Mater. Sci.*, vol. 21, no. 2, pp. 5–15, 2021, doi: 10.2478/adms-2021-0007.
[98] Y. Shao, J. Qi, B. Yuan, L. Li, Wang, and Chao, “Digital Holography Study of the Inhibitory Effects of Polyaspartic Acid on the Anodic Dissolution of Inconel 600,” *Electrochemistry*, vol. 89, no. 3, pp. 267–272, 2021, doi: 10.5796/electrochemistry.21-00021.
[99] M. Znini, “Application of Essential Oils as green corrosion inhibitors for metals and alloys in different aggressive mediums,” *Arab. J. Med. Aromat. Plants*, vol. 5, no. 3, pp. 1–34, 2019, doi: 10.48347/IMIST.PRSM/ajmap-v5i3.18664.
[100] M. Abdallah, I. A. Zaafarany, S. A. El Wanees, and R. Assi, “Corrosion Behavior of Nickel Electrode in NaOH Solution and Its Inhibition by Some Natural Oils,” *Int. J. Electrochem. Sci.*, vol. 9, no. 3, pp. 1071–1086, 2014, doi: 10.1016/S1452-3981(23)07779-9.
[101] M. Abdallah, M. A. Radwan, S. M. Shohayeb, and S. Abdelhamed, “Use of some natural oils as crude pipeline corrosion inhibitors in sodium hydroxide solutions,” *Chem. Technol. Fuels Oils*, vol. 46, no. 5, pp. 354–362, 2010, doi: 10.1007/s10553-010-0234-3.
[102] R. A. Anaee, “Corrosion Inhibition of Monel in 0.2 N HCl Solution by Tris (hydroxymethyl) aminomethane,” *Int. J. Sci. Eng. Res.*, vol. 6, no. 4, pp. 683–686, 2015.
[103] A. Bonk, A. Hanke, M. Braun, W. Ding, and T. Bauer, “Synthetic Biofuels by Molten-Salt Catalytic Conversion: Corrosion of Structural Materials in Ternary Molten Chlorides,” *Adv. Eng. Mater.*, vol. 24, no. 7, p. 2101453, Jul. 2022, doi: 10.1002/adem.202101453.
[104] Y. S. Li and A. Hirose, “Controlled synthesis of diamond and carbon nanotubes on Ni-base alloy,” *Appl. Surf. Sci.*, vol. 255, no. 5, Part 1, pp. 2251–2255, 2008, doi: 10.1016/j.apsusc.2008.07.076.
[105] K. Yamagiwa, “Liquid-phase synthesis of vertically aligned carbon nanotubes and related nanomaterials on preheated alloy substrates,” *Jpn. J. Appl. Phys.*, vol. 57, no. 2S2, p. 02CC07, 2018, doi: 10.7567/JJAP.57.02CC07.
[106] M. V. Lungu *et al.*, “Functional properties improvement of Ag-ZnO thin films using Inconel 600 interlayer produced by electron beam evaporation technique,” *Thin Solid Films*, vol. 667, pp. 76–87, 2018, doi: 10.1016/j.tsf.2018.09.055.
[107] S. Mahini, S. Khameneh Asl, T. Rabizadeh, and H. Aghajani, “Effects of the pack Al content on the microstructure and hot corrosion behavior of aluminide coatings applied on Inconel-600,” *Surf. Coatings Technol.*, vol. 397, p. 125949, 2020, doi: 10.1016/j.surfcoat.2020.125949.
[108] C. B. In, Y. I. Kim, W. W. Kim, J. S. Kim, S. S. Chun, and W. J. Lee, “Pitting resistance and mechanism of TiN-coated Inconel 600 in 100°C NaCl solution,” *J. Nucl. Mater.*, vol. 224, no. 1, pp. 71–78, 1995, doi: 10.1016/0022-3115(95)00033-X.
[109] B. Gregoire, C. Oskay, T. M. Meibner, and M. C. Galetz, “Corrosion performance of slurry aluminide coatings in molten NaCl–KCl,” *Sol. Energy Mater. Sol. Cells*, vol. 223, p. 110974, 2021, doi: 10.1016/j.solmat.2021.110974.
[110] V. Kumar, “Effects of Aging Treatment on Inconel Specimen 600, 625, 718 Coated with Nickel Chromium Carbide (Cr3C2-NiCr) Using Salt and Acidic Corrosion Methods,” 2022, doi: 10.21203/rs.3.rs-2038866/v1.
[111] S. Guo, D. Xu, Y. Li, Y. Guo, S. Wang, and D. D. Macdonald, “Corrosion characteristics and mechanisms of typical Ni-based corrosion-resistant alloys in sub- and supercritical water,” *J. Supercrit. Fluids*, vol. 170, p. 105138, 2021, doi: 10.1016/j.supflu.2020.105138.
[112] A. Kotikian, R. L. Truby, J. W. Boley, T. J. White, and J. A. Lewis, “3D printing of liquid crystal elastomeric actuators with spatially programed nematic order,” *Adv. Mater.*, vol. 30, no. 10, p. 1706164, 2018, doi: 10.1002/adma.201706164.
[113] T. Duan *et al.*, “Long-term field exposure corrosion behavior investigation of 316L stainless steel in the deep sea environment,” *Ocean Eng.*, vol. 189, no. September, p. 106405, 2019, doi: 10.1016/j.oceaneng.2019.106405.
[114] M. Yang *et al.*, “High performance acetone sensor based on ZnO nanorods modified by Au nanoparticles,” *J. Alloys Compd.*, vol. 797, pp. 246–252, 2019, doi: 10.1016/j.jallcom.2019.05.101.
[115] F. Andreatta, A. Lanzutti, E. Vaglio, G. Totis, M. Sortino, and L. Fedrizzi, “Corrosion behaviour of 316L stainless

steel manufactured by selective laser melting," *Mater. Corros.*, vol. 70, no. 9, pp. 1633–1645, 2019, doi: 10.1016/j.egyr.2020.03.029.

[116] Q. W. Ye *et al.*, "Electrochemical behavior of (Cr, W, Al, Ti, Si) N multilayer coating on nitrided AISI 316L steel in natural seawater," *Ceram. Int.*, vol. 46, no. 14, pp. 22404–22418, 2020, doi: 10.1016/j.ceramint.2020.05.323.

[117] L. A. Middlemiss, A. J. R. Rennie, R. Sayers, and A. R. West, "Characterisation of batteries by electrochemical impedance spectroscopy," *Energy Reports*, vol. 6, pp. 232–241, 2020, doi: 10.1016/j.egyr.2020.03.029.

[118] S. Papavinasam, "3 - Electrochemical polarization techniques for corrosion monitoring," in *Woodhead Publishing Series in Metals and Surface Engineering*, L. B. T.-T. for C. M. (Second E. Yang, Ed. Woodhead Publishing, 2021, pp. 45–77. doi: https://doi.org/10.1016/B978-0-08-103003-5.00003-5.

[119] M. Sabzi, S. M. Dezfuli, and Z. Balak, "Crystalline texture evolution, control of the tribocorrosion behavior, and significant enhancement of the abrasion properties of a Ni-P nanocomposite coating enhanced by zirconia nanoparticles," *Int. J. Miner. Metall. Mater.*, vol. 26, pp. 1020–1030, 2019, doi: 10.1007/s12613-019-1805-x.

[120] H. Heo and S. Kim, "Electrochemical Corrosion Damage Characteristics of Austenite Stainless Steel and Nickel Alloy with Various Seawater Concentrations," vol. 20, no. 5, pp. 281–288, 2021, doi: 10.14773/cst.2021.20.5.281.

[121] R. Aslam, "Potentiodynamic polarization methods for corrosion measurement," in *Electrochemical and Analytical Techniques for Sustainable Corrosion Monitoring*, Elsevier, 2023, pp. 25–37. doi: 10.1016/B978-0-443-15783-7.00003-7.

[122] D. H. Abdeen, M. A. Atieh, B. Merzougui, and W. Khalfaoui, "Corrosion Evaluation of 316L Stainless Steel in CNT-Water Nanofluid: Effect of CNTs Loading," *Materials*, vol. 12, no. 10. 2019. doi: 10.3390/ma12101634.

[123] P. Srisungsitthisunti and S. Mahathanabodee, "Surface modification on AISI 316L stainless steels by nanosecond laser with boron nitride powders," *Mater. Today Proc.*, vol. 5, no. 3, Part 2, pp. 9461–9466, 2018, doi: 10.1016/j.matpr.2017.10.125.

[124] N. R. Nik Masdek, N. Wahab, N. Ahmad Nawawi, and A. Tajudin, "The effect of pH on the corrosion rate of 316L Stainless Steel, Nitinol, and Titanium-6% Aluminum-4% Vanadium in Hank's Solution," *Sci. Res. J.*, vol. 18, no. 1, pp. 1–13, 2021.

[125] P. H. Setyarini, F. Gapsari, and A. O. R. Harjo, "Surface Characterization on Electrophoretic Deposition Oof 316l Stainless Steel with Dissolved Chitosan for Biomedical Application," *Int. J. Mech. Eng. Technol. Appl.*, vol. 3, no. 1, pp. 40–46, 2022, doi: 10.21776/MECHTA.2022.003.01.6.

[126] P. Srisungsitthisunti, S. Daopiset, and N. Kanjanaprayut, "Crevice Corrosion of Duplex Stainless Steels by Cyclic Potentiodynamic Polarization and Potentiostatic Techniques," *Key Eng. Mater.*, vol. 728, pp. 123–128, 2017, doi: 10.4028/www.scientific.net/KEM.728.123.

[127] J. T. Ho and G. P. Yu, "Pitting corrosion of inconel 600 in chloride and thiosulfate anion solutions at low temperature," *Corrosion*, vol. 48, no. 2, pp. 147–158, 1992, doi: 10.5006/1.3299821.

[128] W. Tsai, Z.-H. Lee, J.-T. Lee, M.-C. Tsai, and Ping-Holo, "Pitting and stress corrosion cracking behaviour of INCONEL 600 alloy in thiosulphate solution," *Mater. Sci. Eng. A*, vol. 118, pp. 121–129, 1989, doi: 10.1016/0921-5093(89)90064-6.

[129] K. Łyczkowska and J. Michalska, "Studies on the corrosion resistance of laser-welded Inconel 600 and Inconel 625 nickel-based superalloys," *Arch. Metall. Mater.*, vol. 62, 2017, doi: 10.1515/amm-2017-0100.

[130] E.-J. Jung and H.-W. Lee, "Comparison of corrosion resistance and corroded surfaces of welding metal in overlay-welded Inconel 600 and Inconel 625 by gas metal arc welding," *Int. J. Electrochem. Sci*, vol. 11, no. 8, pp. 7125–7138, 2016, doi: 10.20964/2016.08.71.

[131] M. Abdallah, M. M. Salem, I. A. Zaafarany, A. Fawzy, and A. A. A. Fattah, "Corrosion performance of stainless steel and nickel alloys in aqueous sodium hydroxide as revealed from cyclic voltammetry and potentiodynamic anodic polarization," *Orient. J. Chem.*, vol. 33, no. 6, p. 2875, 2017, doi: 10.13005/ojc/330621.

[132] K.-W. Nam, J.-E. Paeng, and K.-Y. Kim, "Immersion Characteristics of STS316L with Degree of Different Cold Rolling," *J. Power Syst. Eng.*, vol. 24, pp. 90–97, Jun. 2020, doi: 10.9726/kspse.2020.24.3.090.

[133] K. Sotoodeh, "Choosing the Right Coating System for Offshore Valves to Prevent

External Corrosion," *J. Bio-and Tribo-Corrosion*, vol. 9, no. 3, p. 55, 2023, doi: 10.1007/s40735-023-00780-7.

[134] S. Gudić, L. Vrsalović, A. Matošin, J. Krolo, E. E. Oguzie, and A. Nagode, "Corrosion Behavior of Stainless Steel in Seawater in the Presence of Sulfide," *Appl. Sci.*, vol. 13, no. 7, 2023, doi: 10.3390/app13074366.

[135] D. Prayitno and J. Riyono," The effect of porosity on the corrosion rate of aluminum foam as a sacrificial anode," *Journal of Integrated and Advanced Engineering (JIAE)*, vol. 4, no. 1, pp. 1-8, 2024, doi: 10.51662/jiae.v4i1.114